Asperindoles A–D and a *p*-Terphenyl Derivative from the Ascidian-Derived Fungus *Aspergillus* sp. KMM 4676

Elena V. Ivanets [1], **Anton N. Yurchenko** [1,*], **Olga F. Smetanina** [1], **Anton B. Rasin** [1], **Olesya I. Zhuravleva** [1,2], **Mikhail V. Pivkin** [1], **Roman S. Popov** [1], **Gunhild von Amsberg** [3], **Shamil Sh. Afiyatullov** [1] and **Sergey A. Dyshlovoy** [1,2,3]

[1] G.B. Elyakov Pacific Institute of Bioorganic Chemistry, Far Eastern Branch of the Russian Academy of Sciences, Prospect 100-letiya Vladivostoka, 159, Vladivostok 690022, Russia; ev.ivanets@yandex.ru (E.V.I.); smetof@rambler.ru (O.F.S.); abrus__54@mail.ru (A.B.R.); zhuravleva.oi@dvfu.ru (O.I.Z.); oid27@mail.ru (M.V.P.); prs_90@mail.ru (R.S.P.); afiyat@piboc.dvo.ru (S.S.A.); dyshlovoy@gmail.com (S.A.D.)

[2] School of Natural Science, Far Eastern Federal University, Sukhanova St., 8, Vladivostok 690000, Russia

[3] Laboratory of Experimental Oncology, Department of Oncology, Hematology and Bone Marrow Transplantation with Section Pneumology, Hubertus Wald-Tumorzentrum, University Medical Center Hamburg-Eppendorf, 20246 Hamburg, Germany; g.von-amsberg@uke.de

* Correspondence: yurchant@ya.ru; Tel.: +7-423-231-1168

Abstract: Four new indole-diterpene alkaloids asperindoles A–D (**1–4**) and the known *p*-terphenyl derivative 3″-hydroxyterphenyllin (**5**) were isolated from the marine-derived strain of the fungus *Aspergillus* sp., associated with an unidentified colonial ascidian. The structures of **1–5** were established by 2D NMR and HRESIMS data. The absolute configurations of all stereocenters of **1–4** were determined by the combination of ROESY data, coupling constants analysis, and biogenetic considerations. Asperindoles C and D contain a 2-hydroxyisobutyric acid (2-HIBA) residue, rarely found in natural compounds. Asperindole A exhibits cytotoxic activity against hormone therapy-resistant PC-3 and 22Rv1, as well as hormone therapy-sensitive human prostate cancer cells, and induces apoptosis in these cells at low-micromolar concentrations.

Keywords: marine-derived fungi; secondary metabolites; indole-diterpenoids; cytotoxicity

1. Introduction

Marine fungi are promising and prolific sources of new biological active compounds. Fungi of the genus *Aspergillus*, section *Candidi* (*A. candidus*, *A. campestris*, *A. taichungensis*, *A. tritici*), are known to produce several types of *p*-terphenyl derivatives, such as terphenyllins (terphenyllin [1], 3-hydroxyterphenyllin [2], terprenins [3]) and candidusins (candidusins A–C [4], prenylcandidusins A–C [5]), and a number of flavonoid derivatives (e.g., chlorflavonin [6], chlorflavonin A [7]). These compounds exhibit antioxidant [8,9], cytotoxic [5,9,10], antimicrobial [9], and immunosuppressive activities [9]. Recently, several indole and pyrrolidine alkaloids unusual for this fungal group were isolated from a Thai sponge-derived *A. candidus* strain [11].

Indole-diterpene alkaloids are widely represented among the fungal metabolites. These compounds have been isolated from fungi of the genera *Claviceps*, *Acremonium*, *Eupenicillium*, *Penicillium*, and *Aspergillus* (including *Emericella striata*). Most natural indole-diterpenes have an invariable framework (Figure 1). Usually, C-7, C-13, and C-27 are oxidized. The oxygenation of C-27 is often followed by the formation of an ether bridge between C-27 and C-7 with inversion of the stereoconfiguration at C-7 [12]. Interestingly, some fungi produce metabolites with relatively

rare features in the classical indole-diterpene backbone. For example, *Acremonium lolii* produces indoles diprenylated at C-20 and C-21, together with oxygenated derivatives [13]. Alkaloids with a 1,3-dioxane moiety joined at C-9 and C-10 with the F-ring from *A. lolii* have also been reported [14,15]. Many of such compounds showed tremorgenic [16], cytotoxic [17,18], and antiinsectan [19] activities, and some of them are antagonists of cannabinoid receptors [20].

Based on promising screening results in search of producers of biologically active compounds, the marine-derived fungus *Aspergillus* sp. KMM 4676, which is associated with an unidentified colonial ascidian (from the Shikotan Island in the Pacific Ocean), was selected for further studies. During earlier examinations of this fungal strain, five known *p*-terphenyls and one known flavonoid were isolated [21]. Herein, we describe the results of subsequent comprehensive chemical and bioactivity investigations of the extracts of strain KMM 4676, leading to the characterization of four new natural compounds.
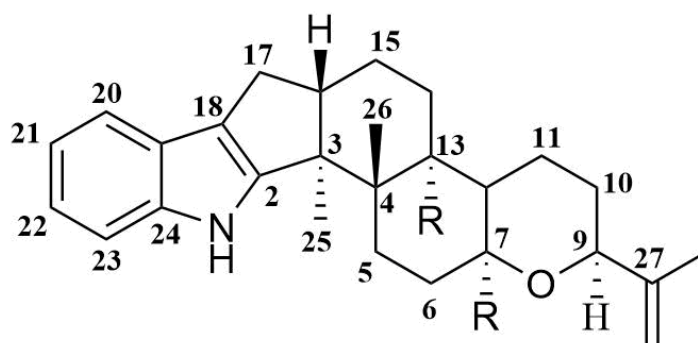
**Figure 1.** Usual framework of indole-diterpenes.

2. Results

The HRESIMS spectrum of **1** exhibited a pseudo-molecular peak at *m/z* 526.1980 [M + H]$^+$, showing the characteristic isotope pattern with one chlorine atom, therefore establishing its molecular formula as $C_{29}H_{32}NO_6Cl$, which was supported by the ^{13}C NMR spectrum.

Inspection of the ^1H and ^{13}C NMR data (Table 1, Figures S1–S2) of **1** revealed the presence of three quaternary methyls (δ_C 16.1, 17.0, 23.4; δ_H 1.02, 1.21, 1.31), one acetate methyl (δ_C 21.8, δ_H 2.07), six methylene sp^3 (δ_C 20.8, 26.3, 26.9, 30.0, 31.5, 64.8; δ_H 1.66, 1.77, 1.91, 1.93, 2.00, 2.11, 2.30, 2.40, 2.55, 2.60, 3.67, 4.04), two methine sp^3 (δ_C 48.3, 78.3, δ_H 2.72, 4.74), four methine sp^2 (δ_C 111.3, 118.6, 118.7, 119.9; δ_H 6.11, 6.91, 7.26, 7.27), three quaternary oxygen-bearing sp^3 (δ_C 75.0, 77.0, 93.6), two quaternary sp^3 (δ_C 38.5, 51.4), and eight quaternary sp^2 (δ_C 115.0, 123.3, 123.7, 140.2, 154.0, 159.1, 170.2, 195.9) carbons, as well as a NH singlet (δ_H 10.73) and an OH singlet (δ_H 5.10).

The ^1H and ^{13}C NMR spectra of **1** (Table 1) resembled those of paspalinine [16], suggesting that **1** has an indole-diterpene core similar to that of paspalinine. However, the differences in chemical shift values of C-19 (δ_C 123.3) and C-22 (δ_C 123.7) of **1** from the corresponding carbons in paspalinine [16]; the HMBC correlations (Figure 2, Figure S5) from H-20 (δ_H 7.26) to C-18 (δ_C 115.0) and C-22, from H-21 (δ_H 7.26) to C-19 and C-23 (δ_C 111.3), and from H-23 (δ_H 7.26) to C-19 and C-21 (δ_C 118.7); and the coupling constants $J_{H20-H21}$ (8.5 Hz) and $J_{H21-H23}$ (2.1 Hz) suggested the presence of a chlorine atom on C-22 of **1**.

Table 1. ^{13}C NMR data (125 MHz, δ in ppm, DMSO-d_6) for asperindoles A–D (**1–4**).

Position	1	2	3	4
2	154.0, C	152.8, C	154.1, C	152.8, C
3	51.4, C	51.2, C	51.4, C	51.2, C
4	38.5, C	38.6, C	38.5, C	38.6, C
5	26.3, CH$_2$	26.2, CH$_2$	26.3, CH$_2$	26.2, CH$_2$
6	30.0, CH$_2$	30.1, CH$_2$	30.0, CH$_2$	30.0, CH$_2$
7	93.6, C	93.6, C	93.6, C	93.5, C
9	78.3, CH	78.3, CH	78.3, CH	78.6, CH
10	195.9, C	195.9, C	195.9, C	195.7, C
11	119.9, CH	119.9, CH	119.9, CH	119.8, CH
12	159.1, C	159.2, C	159.1, C	159.2, C
13	77.0, C	77.0, C	77.0, C	77.0, C
14	31.5, CH$_2$	31.6, CH$_2$	31.5, CH$_2$	31.5, CH$_2$
15	20.8, CH$_2$	20.9, CH$_2$	20.82, CH$_2$	20.9, CH$_2$
16	48.3, CH	48.3, CH	48.3, CH	48.4, CH
17	26.9, CH$_2$	27.1, CH$_2$	26.9, CH$_2$	27.1, CH$_2$
18	115.0, C	114.8, C	115.0, C	114.8, C
19	123.3, C	124.6, C	123.3, C	124.6, C
20	118.6, CH	117.5, CH	118.6, CH	117.5, CH
21	118.7, CH	118.3, CH	118.7, CH	118.3, CH
22	123.7, C	119.1, CH	123.7, C	119.1, CH
23	111.3, CH	111.8, CH	111.3, CH	111.8, CH
24	140.2, C	139.9, C	140.2, C	139.9, C
25	16.1, CH$_3$	16.2, CH$_3$	16.1, CH$_3$	16.2, CH$_3$
26	23.4, CH$_3$	23.4, CH$_3$	23.4, CH$_3$	23.3, CH$_3$
27	75.0, C	75.0, C	75.8, C	75.8, C
28	64.8, CH$_2$	64.8, CH$_2$	64.1, CH$_2$	64.1, CH$_2$
29	17.0, CH$_3$	17.0, CH$_3$	16.4, CH$_3$	16.4, CH$_3$
1′	170.2, C	170.2, C	171.1, C	171.1, C
2′	21.8, CH$_3$	21.8, CH$_3$	77.9, C	77.9, C
3′			23.9, CH$_3$	23.9, CH$_3$
4′			24.2, CH$_3$	24.2, CH$_3$
1″			169.3, C	169.3, C
2″			20.75, CH$_3$	20.8, CH$_3$
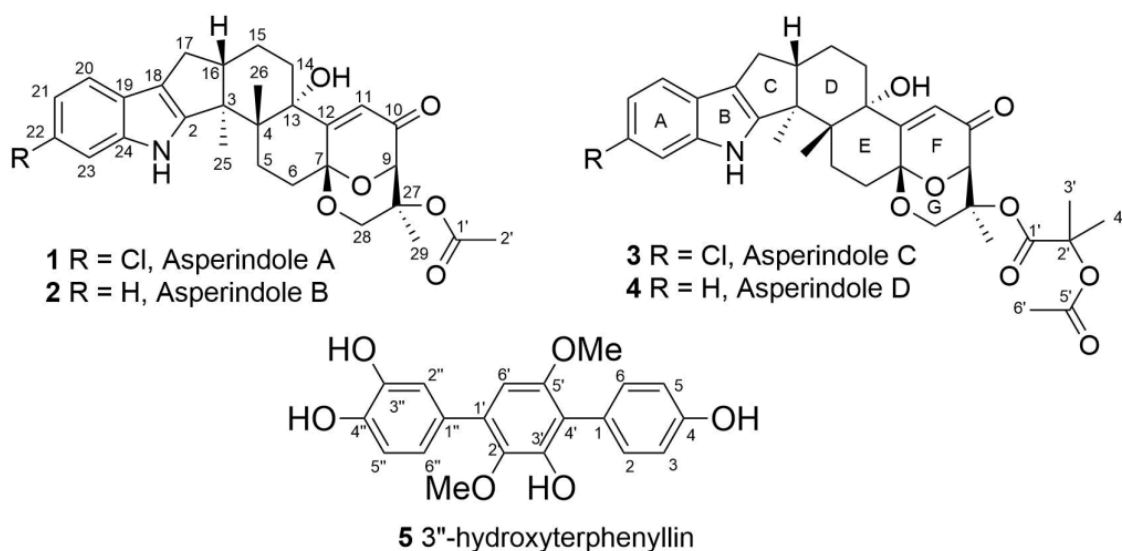
Figure 2. Chemical structures of **1–5**.

The HMBC correlations (Figure 3, Figure S5) from H-28β (δ_H 3.67) to C-27 (δ_C 75.0), C-29 (δ_C 17.0), and C-1′ (δ_C 170.2); from H-9 (δ_H 4.74) to C-7 (δ_C 93.6), C-28 (δ_C 64.8), and C-27; from H-28α (δ_H 4.04) to C-7, C-9 (δ_C 78.3), and C-27; and from H$_3$-29 (δ_H 1.21) to C-27 suggested the presence of a 1,3-dioxane ring with an acetoxy group at C-27. The W-type coupling constant $J_{H9-H28\alpha}$ (2.5 Hz) and ROESY correlations (Figure 4, Figure S6) of H-28β with H-11 (δ_H 6.11), H$_3$-29, H$_3$-26 (δ_H 1.02), and of H-28α with H$_3$-29 indicated a relative configuration of chiral centers in the 1,3-dioxane ring as 7*R**, 9*R**, 27*S**. The ROESY correlations (Figure 4, Figure S6) of H$_3$-25 (δ_H 1.31) with H-5α (δ_H 1.93), 13-OH (δ_H 5.10), H-6α (δ_H 2.00), and H-15α (δ_H 1.91), and of H-16 (δ_H 2.72) with H$_3$-26 (δ_H 1.02) suggested the relative configurations of the stereogenic carbons of the C–G rings in **1** as 3*S**, 4*R**, 13*S**, 16*R**. The absolute configurations of all stereocentres in **1** was proposed as 3*S*, 4*R*, 7*R*, 9*R*, 13*S*, 16*R*, 27*S*—the same as those in paspalinine—based on biosynthetic considerations, and was confirmed by the comparison of the ECD (electronic circular dichroism) spectral data with that of paspalinine [17] (Figure 5). Compound **1** was named asperindole A. It should be noted that chlorinated indolediterpenes are rare in nature [12,22–25].
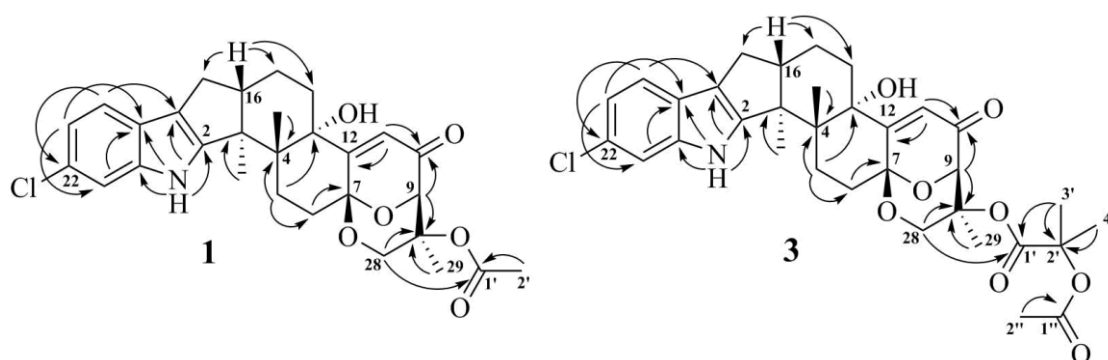

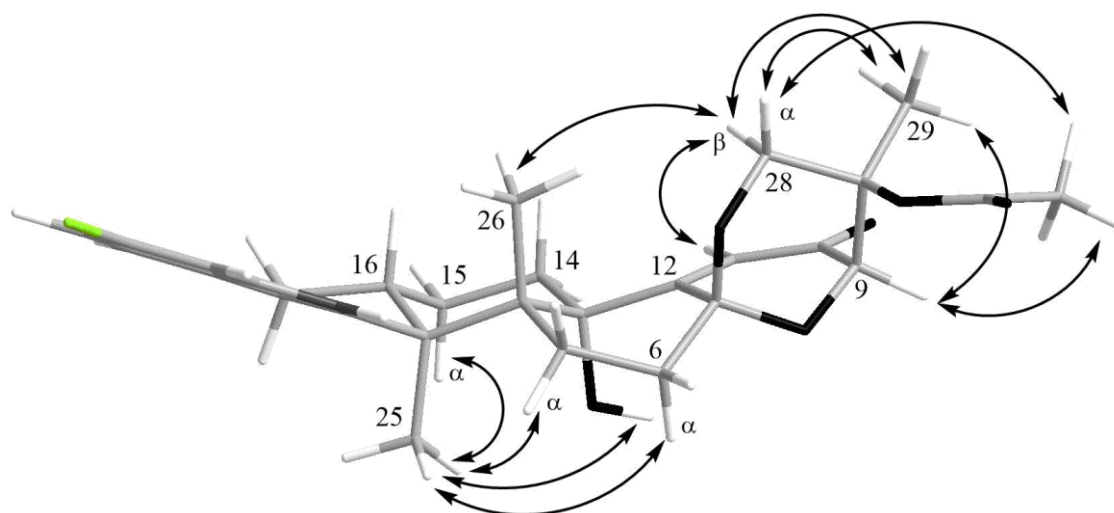**Figure 3.** Key HMBC correlations of **1** and **3**.

Figure 4. Key ROESY correlations in asperindole A (**1**).

The molecular formula of **2** was determined as C$_{29}$H$_{33}$NO$_6$ by a HRESIMS peak at *m/z* 490.2188 [M − H]$^-$, which was supported by the ^{13}C NMR spectrum. The general features of the ^{1}H and ^{13}C NMR spectra (Table 1, Figures S7 and S8) of **2** resemble those of **1**, with the exception of the proton and carbon signals of an indole moiety, as well as the absence of a chlorine atom as evidenced by the HRESIMS spectrum. The coupling constants and the multiplicity of the aromatic protons in ring A (H-20, δ_H 7.25, d, *J* = 7.6 Hz; H-21, δ_H 6.89, t, *J* = 7.6 Hz; H-22, δ_H 6.93, t, *J* = 7.6 Hz; and H-23, δ_H 7.27,

d, *J* = 7.6 Hz) allowed the conclusion to be made that **2** is a nonchlorinated analogue of **1**. Compound **2** was therefore named asperindole B.

The molecular formula of **3** was established as $C_{33}H_{38}NO_8Cl$ on the basis of the HRESIMS, containing a peak at *m/z* 610.2206 [M − H]⁻, and was supported by the ^{13}C NMR spectrum. The analysis of the NMR data (Figures S14–S20) for **3** revealed the presence of the same indole-diterpene framework as that in **1**, with the exception of the proton and carbon signals in a 1,3-dioxane ring, as well as the presence of two methyl (δ_C 23.9, 24.2), an ester carbonyl (δ_C 171.1), and an oxygen-bearing quaternary *sp*³ (δ_C 77.9) carbons. The HMBC correlations (Figure 3, Figure S19) from H-3′ (δ_H 1.52) and H-4′ (δ_H 1.54) to C-2′ (δ_C 77.9), and from H-6′ (δ_H 2.04) to C-5′ (δ_C 169.3) suggested the presence of an acetylated residue of 2-hydroxyisobutyric acid (2-HIBA) in **3**. This was corroborated by the molecular weight of **3**, which was 86 amu ($C_4H_6O_2$) greater than that of **1**. The ROESY correlations of **3** (Figure S20) were similar to those in **1** (Figure 4, Figure S6). Based on these data and together with the ECD spectrum of **1** (Figure 5), the absolute configurations of all stereocentres in **3** were proposed to be the same as those in asperindole A. Consequently, **3** was named asperindole C. To the best of our knowledge, the 2-HIBA residue is unique amongst naturally occurring compounds.
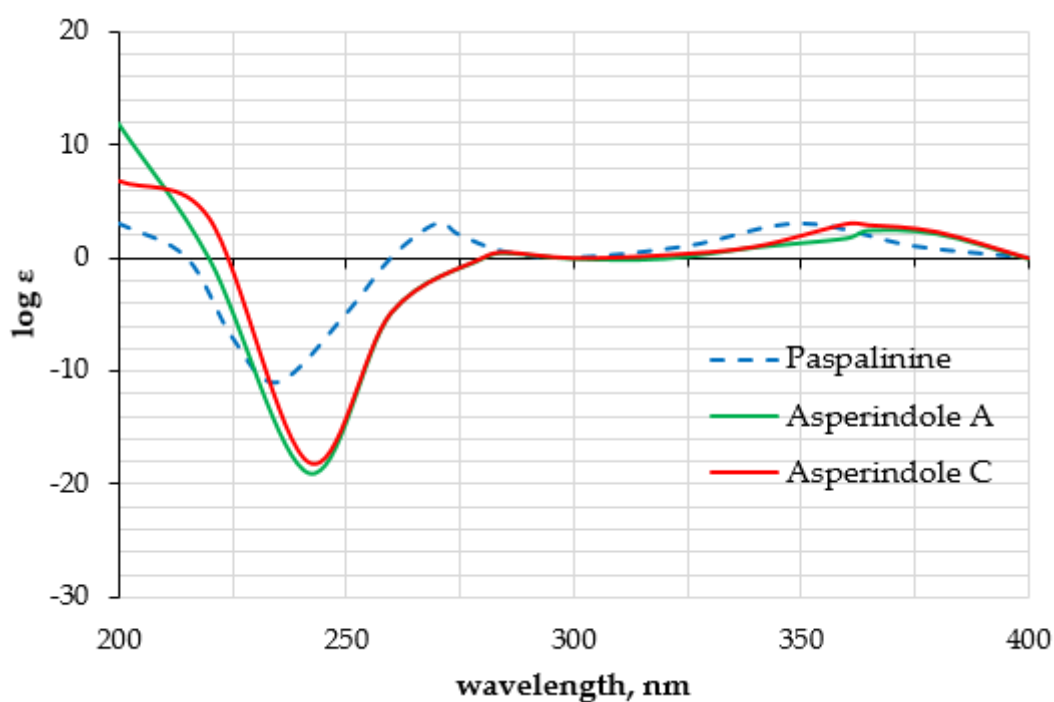

Figure 5. Experimental ECD data of **1**, **3**, and paspalinine [17].

The HRESIMS spectrum of **4** exhibited the [M − H]⁻ peak at *m/z* 576.2594, corresponding to $C_{33}H_{39}NO_8$, which was supported by the ^{13}C NMR spectrum. The general features of the ^{1}H and ^{13}C NMR spectra (Table 2, Figures S21 and S22) of **4** resembled those of **3**, with the exception of some proton and carbon signals of the indole moiety. Similar to **2**, the coupling constants and multiplicity of the aromatic protons in ring A (H-20, δ_H 7.25, d, *J* = 7.5 Hz; H-21, δ_H 6.88, brt, *J* = 7.2 Hz; H-22, δ_H 6.92, brt, *J* = 7.1 Hz; and H-23, δ_H 7.27, d, *J* = 6.9 Hz) led to the conclusion that **4** is a nonchlorinated analogue of **3**. Compound **4** was therefore named asperindole D.

Table 2. ^{1}H NMR data (δ in ppm, *J* in Hz, DMSO-d_6) for asperindoles A–D (**1–4**).

Position	1 *	2 **	3 **	4 **
NH	10.73, brs	10.54, brs	10.73, s	10.52, s
5α	1.93, m	1.96, m	1.95, m	1.96, m
5β	2.40, dd (13.4, 10.0)	2.41, t (12.3)	2.39, dd (13.4,10.0)	2.41, t (12.3)
6α	2.00, dd (12.9, 8.6)	1.99, m	1.95, dd (12.9, 8.6)	1.95, dd (12.9, 8.6)
6β	2.55, m	2.55, m	2.55, m	2.55, m
9	4.74, d (2.3)	4.74, d (2.1)	4.74, d (2.3)	4.63, d (2.4)
11	6.11, s	6.11, s	6.11, s	6.12, s
14α	2.11, dt (13.6, 2.8)	2.12, brd (13.4)	2.12, dt (13.6, 2.8)	
14β	1.77, td (13.2, 4.5)	1.78, brt (13.4)	1.76, td (13.2, 4.5)	
15α	1.91, m	1.91, m	1.91, m	1.91, m
15β	1.66, m	1.66, m	1.65, m	1.65, m
16	2.72, m	2.72, m	2.72, m	2.63, m
17α	2.30, dd (13.0, 10.9)	2.30, t (12.3)	2.30, dd (13.0, 10.9)	2.31, dd (13.0, 10.9)
17β	2.60, dd (13.0, 6.4)	2.60, dd (12.3, 6.6)	2.60, dd (13.0, 6.4)	2.60, dd (13.0, 6.2)
20	7.26, d (8.6)	7.25, d (7.6)	7.26, d (8.3)	7.25, d (7.5)
21	6.91, dd (8.3, 1.9)	6.89, t (7.6)	6.91, dd (8.3, 2.0)	6.88, brt (7.2)
22		6.93, t (7.6)		6.92, brt (7.1)
23	7.27, d (2.2)	7.27, d (7.6)	7.25, d (2.0)	7.27, d (6.9)
25	1.31, s	1.30, s	1.31, s	1.30, s
26	1.02, s	1.03, s	1.02, s	1.03, s
28α	4.04, dd (13.4, 2.5)	4.05, dd (13.3, 2.1)	4.11, dd (13.2, 2.5)	4.11, dd (13.4, 2.4)
28β	3.67, d (13.4)	3.68, d (13.3)	3.68, d (13.2)	3.69, d (13.4)
29	1.21, s	1.21, s	1.17, s	1.18, s
3$'$			1.52, s	1.52, s
4$'$			1.54, s	1.54, s
2$''$	2.07, s	2.07, s	2.04, s	2.04, s
13-OH	5.10, s	5.08, s	5.11, s	5.08, s

^{1}H NMR spectroscopic data were measured at * 700 MHz and ** 500 MHz, respectively.

The molecular formula of **5** was determined as $C_{20}H_{18}O_6$, based on a pseudo-molecular peak at *m/z* 353.1013 [M − H]$^-$ from the HRESIMS spectrum. This was supported by the ^{13}C NMR spectrum. A close inspection of the ^{1}H and ^{13}C NMR data (Table 3, Figures S23 and S24) of **5** revealed the presence of eight aromatic protons (δ_H 6.47, 6.85, 2H; 6.91, 7.02, 7.19, 7.25, 2H) and eight methine sp^2 (δ_C 104.8, 115.9, 115.9, 116.8, 117.5, 122.0, 133.7, 133.7), six oxygen-bearing quaternary sp^2 (δ_C 140.8, 146.3, 146.4, 149.8, 155.1, 157.6), and four quaternary sp^2 (δ_C 118.3, 126.8, 131.9, 134.2) carbons, and two methoxy groups (δ_C 56.8, 61.4; δ_H 3.41, 3.71). A direct comparison of ^{1}H and ^{13}C NMR spectra of **5** (Table 3, Figures S23 and S24) with those of terphenyllin [1] showed their close resemblance, with the exception of the presence of a hydroxy group at C-3$''$ (δ_C 146.4) and the difference in carbon chemical shifts at C-2$''$ (δ_C 117.5), C-4$''$ (δ_C 146.3), C-5$''$ (δ_C 116.8) and C-6$''$ (δ_C 122.0) (131.1 ppm for C-1$''$, C-2$''$, and C-6$''$; 158.0 ppm for C-4$''$ in terphenyllin [1]). The HMBC correlations (Figure 6, Figure S27) from H-2 (δ_H 7.25) to C-4 (δ_C 157.6), C-6 (δ_C 133.7), and C-4$'$ (δ_C 118.3); from H-3 (δ_H 6.85) to C-1 (δ_C 126.8) and C-5 (δ_C 115.9); from H-5 (δ_H 6.85) to C-3 (δ_C 115.9) and C-1; from H-6 (δ_H 7.25) to C-2 (δ_C 133.7), C-4, and C-4$'$; from H-6$'$ (δ_H 6.47) to C-2$'$ (δ_C 140.8), C-4$'$, and C-1$''$ (δ_C 131.9); from H-2$''$ (δ_H 7.19) to C-1$'$ (δ_C 134.2), C-4$''$, and C-6$''$; from H-5$''$ (δ_H 6.91) to C-1$''$ and C-3$''$; from H-6$''$ (δ_H 7.50) to C-1$'$, C-2$''$, and C-4$''$; and ROESY correlation from H-6$'$ and 2$'$-OMe (δ_H 3.41) to H-2$''$ and H-6$''$, and from 5$'$-OMe (δ_H 3.71) to H-2 (H-6) established the structure of **5** as the 2$'$,5$'$-dimethoxy-4,3$'$,3$''$,4$''$-tetrahydroxy-*p*-terphenyl derivative. This structure was previously published as hydroxyterphenyllin in an unavailable source [26]. It should be noted that these authors reported the name "hydroxyterphenyllin" for an isomeric compound [27] now known as 3-hydroxyterphenyllin [2,28]. Probably, the structure of **5** was mistakenly provided by [26] instead of the structure of 3-hydroxyterphenyllin. Therefore, **5** should be named 3$''$-hydroxyterphenyllin.
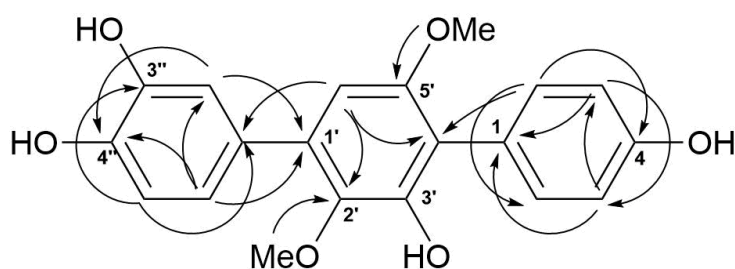
Figure 6. Key HMBC correlations of **5**.

Table 3. ^{1}H and ^{13}C NMR data (δ in ppm, DMSO-d_6) for 3″-hydroxyterphenyllin (**5**).

Position	δ_C, mult	δ_H (*J* in Hz)	HMBC	ROESY
1	126.8, C			
2	133.7, CH	7.25, d (8.4)	4, 6, 4′	
3	115.9, CH	6.85, d (8.5)	1, 5	
4	157.6, C			
5	115.9, CH	6.85, d (8.5)	1, 3	
6	133.7, CH	7.25, d (8.4)	2, 4, 4′	5′-OMe
1′	134.2, C			
2′	140.8, C			
3′	149.8, C			
4′	118.3, C			
5′	155.1, C			
6′	104.8, CH	6.47, s	2′, 4′, 1″	2″, 6″
1″	131.9, C			
2″	117.5, CH	7.19, d (2.1)	1′, 4″, 6″	6′, 2′-OMe
3″	146.4, C			
4″	146.3, C			
5″	116.8, CH	6.91, d (8.1)	1″, 3″	
6″	122.0, CH	7.02, dd (8.1, 2.1)	1′, 2″, 4″	6′, 2′-OMe
2′-OMe	61.4, CH$_3$	3.41, s	2′	2″, 6″
5′-OMe	56.8, CH$_3$	3.71, s	5′	6

^{1}H NMR and ^{13}C NMR spectroscopic data were measured at 700 MHz and 175 MHz, respectively.

The biosynthesis of related indole-diterpenes was previously proposed for paspalinine [29]. Apparently, the common biosynthetic precursor of asperindoles and 1,3-dioxolane indole-diterpenoids (including paspalinine) is 7α-hydroxypaxilline (Figure 7). Oxidation of the isopropyl substituent, followed by cyclization at C-7 and C-2′, generates a 1,3-dioxane ring. Asperindoles are then formed by acylation and halogenation.

The effect of the asperindoles A (**1**) and C (**3**) on cell viability, cell cycle progression, and induction of apoptosis in human prostate cancer cell lines was investigated. MTT assays revealed that asperindole C (**3**) was noncytotoxic against human PC-3, LNCaP (androgen-sensitive human prostate adenocarcinoma cells), and 22Rv1 cell lines with an IC$_{50}$ > 100 μM. In contrast, asperindole A (**1**) showed cytotoxicity in all three cell lines, with IC$_{50}$ values of 69.4 μM, 47.8 μM, and 4.86 μM, respectively. Docetaxel, which was used as a reference substance, displayed IC$_{50}$ values of 15.4 nM, 3.8 nM, and 12.7 nM, respectively. Asperindole A (**1**) was able to induce apoptosis in human cancer 22Rv1 cells at low-micromolar concentrations (Figure 8). Cell cycle progression analysis of 22Rv1 cells treated with asperindole A (**1**) for 48 h revealed a S-phase arrest (as well as a discrete G2/M-phase arrest, Figure 8). Thus, asperindole A (**1**) may be a promising candidate for further studies in human drug-resistant prostate cancer. In contrast, 22Rv1 cells treated with 100 μM of asperindole C (**3**) for 48 h revealed only minimal induction of apoptosis (8.9 ± 0.6% vs 1.2 ± 0.1% in the control) and no significant changes in cell cycle progression.

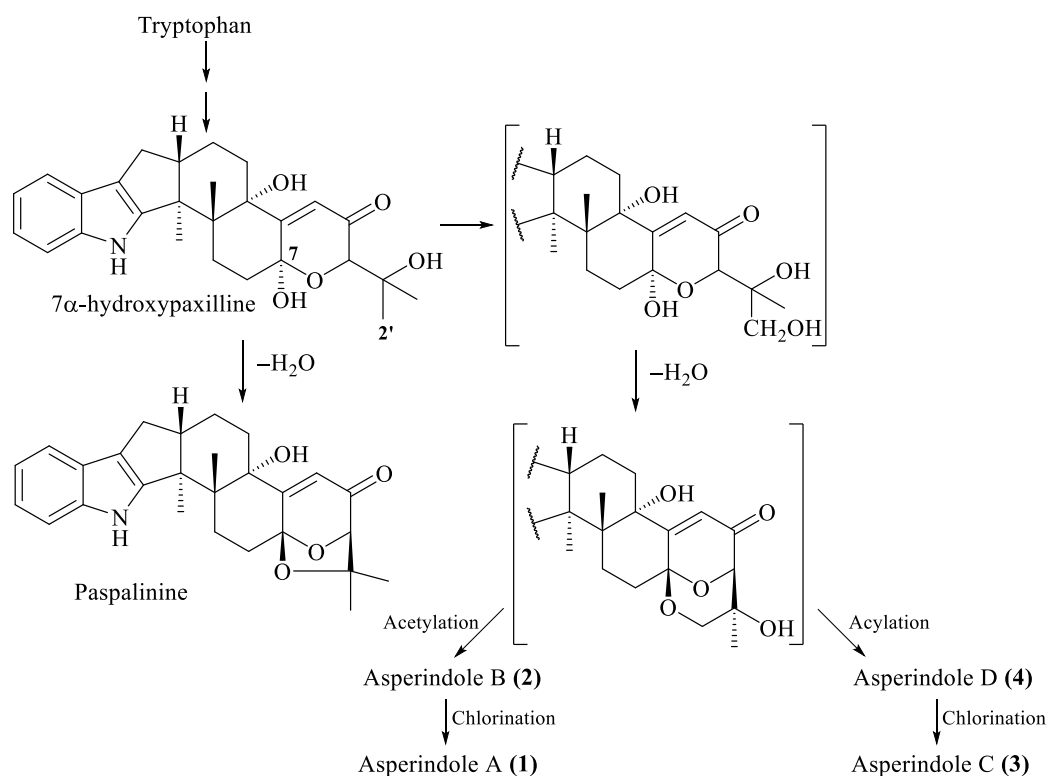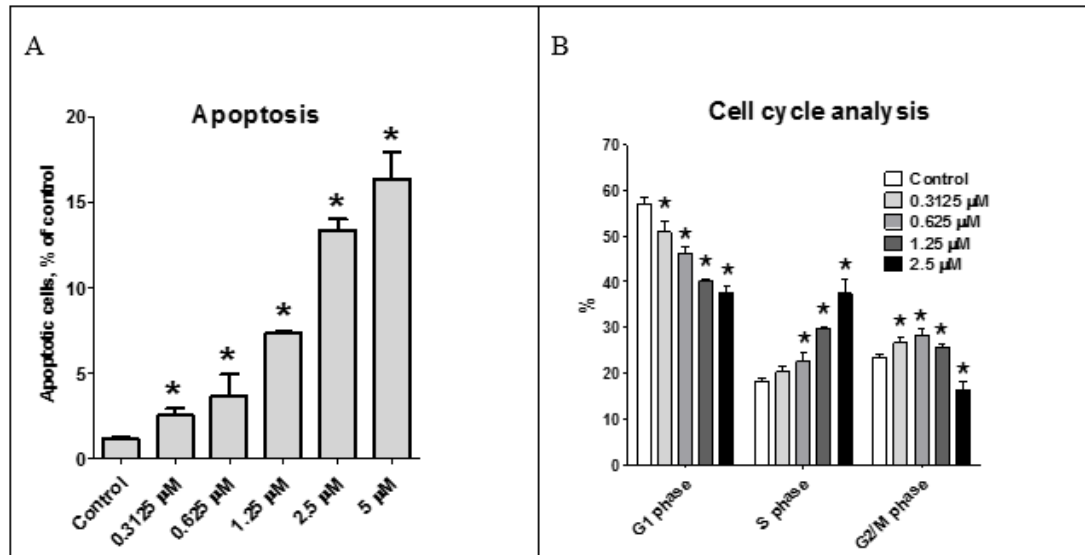**Figure 7.** Proposed biosynthesis of asperindoles A–D (**1**–**4**).

Figure 8. Effect of asperindole A (**1**) on cell cycle progression and apoptosis induction. Apoptotic cells were detected as a sub-G1 population (**A**); Cell cycle analysis of 22Rv1 cells treated with asperindole A (**1**) for 48 h (**B**). Cell cycle phase distribution, quantified using the Cell Quest Pro software. * $p < 0.05$.

3. Materials and Methods

3.1. General Experimental Procedures

Optical rotations were measured on a Perkin-Elmer 343 polarimeter (Perkin Elmer, Waltham, MA, USA). UV spectra were recorded on a Specord UV−vis spectrometer (Carl Zeiss, Jena, Germany)

in $CHCl_3$. NMR spectra were recorded in DMSO-d_6 on a Bruker DPX-500 (Bruker BioSpin GmbH, Rheinstetten, Germany) and a Bruker DRX-700 (Bruker BioSpin GmbH, Rheinstetten, Germany) spectrometer, using TMS as an internal standard. HRESIMS spectra were measured on an Agilent 6510 Q-TOF LC mass spectrometer (Agilent Technologies, Santa Clara, CA, USA) and a Maxis impact mass spectrometer (Bruker Daltonics GmbH, Rheinstetten, Germany).

Low-pressure liquid column chromatography was performed using silica gel (50/100 μm, Imid, Russia). Plates (4.5 cm × 6.0 cm) precoated with silica gel (5–17 μm, Imid) were used for thin-layer chromatography. Preparative HPLC was carried out on a Shimadzu LC-20 chromatograph (Shimadzu USA Manufacturing, Canby, OR, USA) using a YMC ODS-AM (YMC Co., Ishikawa, Japan) (5 μm, 10 mm × 250 mm) and YMC SIL (YMC Co., Ishikawa, Japan) (5 μm, 10 mm × 250 mm) columns with a Shimadzu RID-20A refractometer (Shimadzu Corporation, Kyoto, Japan).

3.2. Fungal Strain

The strain was isolated from an unidentified colonial ascidian (Shikotan Island, Pacific Ocean) on malt extract agar, and identified on the basis of morphological and molecular features. For DNA extraction, the culture was grown on malt extract agar under 25 °C for 7 days. DNA extraction was performed with the HiPurATM Plant DNA Isolation kit (CTAB Method) (HiMedia Laboratories Pvt. Ltd., Mumbai, India) according to the manufacturer's instructions. Fragments containing the ITS (internal transcribed spacer) regions were amplified using ITS1 and ITS4 primers. The newly obtained sequences were checked visually and compared to available sequences in the GenBank database (www.mycobank.org). According to BLAST analysis of the ITS1–5.8S–ITS2 sequence, the strain KMM 4676 had 98% similarity with *Aspergillus candidus.* The sequences were deposited in the GenBank nucleotide sequence database under MG 241226. The strain is deposited in the Collection of Marine Microorganisms of G. B. Elyakov Pacific Institute of Bioorganic Chemistry FEB RAS under the code KMM 4676.

3.3. Cultivation of Fungus

The fungus was cultured at 22 °C for three weeks in 14 × 500 mL Erlenmeyer flasks, each containing rice (20.0 g), yeast extract (20.0 mg), KH_2PO_4 (10 mg), and natural sea water (40 mL).

3.4. Extraction and Isolation

The fungal mycelia with the medium were extracted for 24 h with 5.6 L of EtOAc. Evaporation of the solvent under reduced pressure gave a dark brown oil (6.25 g), to which 250 mL H_2O–EtOH (4:1) was added, and the mixture was thoroughly stirred to yield a suspension. It was extracted successively with *n*-hexane (150 mL × 2), EtOAc (150 mL × 2), and *n*-BuOH (150 mL × 2). After evaporation of the EtOAc layer, the residual material (3.92 g) was passed over a silica gel column (35.0 cm × 2.5 cm, 75 g), which was eluted first with *n*-hexane (1.0 L), followed by a step gradient from 5% to 100% EtOAc in *n*-hexane (total volume 30 L). Fractions of 250 mL each were collected and combined on the basis of TLC (Si gel, toluene–2-propanol, 6:1 and 3:1, *v/v*).

The *n*-hexane–EtOAc (9:1, 2 L, 21.70 mg) fraction was purified by LH-20 column (80 cm × 2 cm, 50 g) with $CHCl_3$ to yield 30 subfractions. Subfraction 6 is the individual compound **1** (8.30 mg). Subfractions 8–12 (7.00 mg) were purified by HPLC on a YMC ODS-AM column, eluting with MeOH–H_2O (9:1), and then by HPLC on a YMC SIL column, eluting with acetone–*n*-hexane (1:3) to yield **2** (0.56 mg), **3** (1.05 mg), and **4** (1.47 mg). The *n*-hexane–EtOAc (4:1, 2 L, 145 mg) fraction was purified by by HPLC on a YMC ODS-AM column, eluting with MeOH–H_2O (13:7), then by HPLC on a YMC-SIL column eluting first with $CHCl_3$–MeOH–NH_4OAc (90:10:1.5), and then with $CHCl_3$–MeOH–NH_4OAc (85:15:1) to yield **5** (56.10 mg).

Asperindole A (**1**): white powder; $[\alpha]_D^{20}$ +22 (*c* 0.10, $CHCl_3$); UV (MeOH) λ_{max} (log ε) 284 (3.86), 236.4 (4.55), 195.6 (4.55) nm; ECD (0.21 mM, MeOH) λ_{max} (Δε) 205 (+8.52), 240 (−19.80), 280 (+0.25),

360 (+3.60) nm; ^{1}H and ^{13}C NMR data see Table 1, Figures S1–S6; HR ESIMS *m/z* 526.1980 [M + H]$^+$ (calcd. for $C_{29}H_{33}NO_6Cl$, 526.1992, Δ −2.28 ppm).

Asperindole B (**2**): white powder; $[\alpha]_D^{20}$ +40 (*c* 0.03, CHCl$_3$); ^{1}H and ^{13}C NMR data see Table 1, Figures S7–S13; HRESIMS *m/z* 514.2194 [M + Na]$^+$ (calcd. for $C_{29}H_{33}NO_6Na$, 514.2200, Δ −1.17 ppm).

Asperindole C (**3**): white powder; $[\alpha]_D^{20}$ +46 (*c* 0.72, CHCl$_3$); UV (MeOH) λ_{max} (log ε) 284 (3.90), 236.4 (4.56), 194.8 (4.46) nm; ECD (0.21 mM, MeOH) λ_{max} ($\Delta\varepsilon$) 205 (+6.43), 240 (−18.25), 280 (+0.02), 360 (+3.57) nm; ^{1}H and ^{13}C NMR data see Table 2, Figures S14–S20; HRESIMS *m/z* 610.2206 [M − H]$^-$ (calcd. for $C_{33}H_{37}NO_8Cl$, 610.2213, Δ −1.15 ppm).

Asperindole D (**4**): white powder; $[\alpha]_D^{20}$ +24 (*c* 0.05, CHCl$_3$); ^{1}H and ^{13}C NMR data, see Table 2, Figures S21 and S22; HRESIMS *m/z* 576.2594 [M − H]$^-$ (calcd. for $C_{33}H_{38}NO_8$, 576.2603, Δ −1.56 ppm).

3″-hydroxyterphenylline (**5**)*:* ^{1}H and ^{13}C NMR data, see Table 3, Figures S23–S27; HRESIMS *m/z* 353.1036 [M − H]$^-$ (calcd. for $C_{20}H_{17}O_6$, 353.1031, Δ −1.42 ppm).

3.5. Cell Culture

The human prostate cancer cells lines 22Rv1, PC-3, and LNCaP were purchased from ATCC. Cell lines were cultured in 10% FBS/RPMI media (Invitrogen Ltd., Paisley, UK) with (for LNCaP) or without (for 22Rv1 and PC-3) 1 mM sodium pyruvate (Invitrogen). Cells were continuously kept in culture for a maximum of 3 months, and were routinely inspected microscopically for stable phenotype and regularly checked for contamination with mycoplasma. Cell line authentication was performed by DSMZ (Braunschweig, Germany) using highly polymorphic short tandem repeat loci [30].

3.6. Cytotoxicity Assay

The in vitro cytotoxicity of individual substances was evaluated using the MTT (3-(4,5-dimethylthiazol-2-yl)-2,5-diphenyltetrazolium bromide) assay, which was performed as previously described [31]. Docetaxel was used as a control.

3.7. Cell Cycle and Apoptosis Induction Analysis

The cell cycle distribution was analyzed by flow cytometry using PI (propidium iodide) staining as described before with slight modifications [32]. In brief, cells were preincubated overnight in 6-well plates (2×10^5 cells/well in 2 mL/well). The medium was changed to fresh medium containing different concentrations of the substances. After 48 h of treatment, cells were harvested with a trypsin-EDTA solution, fixed with 70% EtOH, stained, and analyzed by BD Bioscience FACS Calibur analyzer (BD Bioscience, Bedford, MA, USA). The results were quantitatively analyzed using BD Bioscience Cell Quest Pro v.5.2.1. software (San Jose, CA, USA). Cells detected in the sub-G1 peak were considered as apoptotic.

4. Conclusions

Four new metabolites, the indole-diterpene alkaloids asperindoles A–D (**1–4**), and the known *p*-terphenyl derivative 3″-hydroxyterphenyllin (**5**) were isolated from a marine-derived strain of the fungus *A. candidus* KMM 4676, associated with an unidentified colonial ascidian. To the best of our knowledge, **3** and **4** are the first examples of naturally occurring compounds containing a 2-hydroxyisobutiric acid (2-HIBA) residue. This is the first report of the spectral data and reliable assignment for 3″-hydoxyterphenyllin (**5**). Asperindole A (**1**) was proved to be highly cytotoxic in 22Rv1 human prostate cancer cells resistant to androgen receptor-targeted therapies. Therefore, this compound is a promising candidate for further evaluation in human drug-resistant prostate cancer cells.

References

1. Marchelli, R.; Vining, L.C. Terphenyllin, a novel p terphenyl metabolite from *Aspergillus candidus*. *J. Antibiot.* **1975**, *28*, 328–331. [CrossRef] [PubMed]

2. Kurobane, I.; Vining, L.C.; McInnes, A.G.; Smith, D.G. 3-Hydroxyterphenyllin, a new metabolite of *Aspergillus candidus*. Structure elucidation by 1H and 13C nuclear magnetic resonance spectroscopy. *J. Antibiot.* **1979**, *32*, 559–564. [CrossRef] [PubMed]

3. Kamigauchi, T.; Sakazaki, R.; Nagashima, K.; Kawamura, Y.; Yasuda, Y.; Matsushima, K.; Tani, H.; Takahashi, Y.; Ishii, K.; Suzuki, R.; et al. Terprenins, novel immunosuppressants produced by *Aspergillus candidus*. *J. Antibiot.* **1998**, *51*, 445–450. [CrossRef] [PubMed]

4. Rahbæk, L.; Frisvad, J.C.; Christophersen, C. An amendment of *Aspergillus* section *Candidi* based on chemotaxonomical evidence. *Phytochemistry* **2000**, *53*, 581–586. [CrossRef]

5. Cai, S.; Sun, S.; Zhou, H.; Kong, X.; Zhu, T.; Li, D.; Gu, Q. Prenylated polyhydroxy-p-terphenyls from *Aspergillus taichungensis* ZHN-7-07. *J. Nat. Prod.* **2011**, *74*, 1106–1110. [CrossRef] [PubMed]

6. Bird, A.E.; Marshall, A.C. Structure of chlorflavonin. *J. Chem. Soc. C* **1969**, *18*, 2418–2420. [CrossRef]

7. Yan, T.; Guo, Z.K.; Jiang, R.; Wei, W.; Wang, T.; Guo, Y.; Song, Y.C.; Jiao, R.H.; Tan, R.X.; Ge, H.M. New Flavonol and Diterpenoids from the Endophytic Fungus *Aspergillus* sp. YXf3. *Planta Med.* **2013**, *79*, 348–352. [CrossRef] [PubMed]

8. Kuhnert, E.; Surup, F.; Herrmann, J.; Huch, V.; Müller, R.; Stadler, M.; Rickenyls, A.-E. antioxidative terphenyls from the fungus Hypoxylon rickii (Xylariaceae, Ascomycota). *Phytochemistry* **2015**, *118*, 68–73. [CrossRef] [PubMed]

9. Valeria Calì, C.S.; Tringali, C. Polyhydroxy-P-Terphenyls and Related P-Terphenylquinones From Fungi: Overview and Biological Properties. *Stud. Nat. Prod. Chem.* **2003**, *29*, 263–307.

10. Kobayashi, A.; Takemoto, A.; Koshimizu, K.; Kawazu, K. p-Terphenyls with cytotoxic activity toward sea urchin embryos. *Agric. Biol. Chem.* **1985**, *49*, 867–868. [CrossRef]

11. Buttachon, S.; Ramos, A.A.; Inácio, Â.; Dethoup, T.; Gales, L.; Lee, M.; Costa, P.M.; Silva, A.M.S.; Sekeroglu, N.; Rocha, E.; et al. Bis-indolyl benzenoids, hydroxypyrrolidine derivatives and other constituents from cultures of the marine sponge-associated fungus *Aspergillus candidus* KUFA0062. *Mar. Drugs* **2018**, *16*, 119. [CrossRef] [PubMed]

12. Netz, N.; Opatz, T. Marine indole alkaloids. *Mar. Drugs* **2015**, *13*, 4814–4914. [CrossRef] [PubMed]

13. Munday-Finch, S.C.; Miles, C.O.; Wilkins, A.L.; Hawkes, A.D. Isolation and Structure Elucidation of Lolitrem A, a Tremorgenic Mycotoxin from *Perennial Ryegrass* Infected with *Acremonium lolii*. *J. Agric. Food Chem.* **1995**, *43*, 1283–1288. [CrossRef]

14. Gallagher, R.T.; White, E.P.; Mortimer, P.H. Ryegrass staggers: Isolation of potent neurotoxins lolitrem a and lolitrem b from staggers-producing pastures. *N. Z. Vet. J.* **1981**, *29*, 189–190. [CrossRef] [PubMed]

15. Munday-Finch, S.C.; Wilkins, A.L.; Miles, C.O.; Tomoda, H.; Omura, S. Isolation and Structure Elucidation of Lolilline, a Possible Biosynthetic Precursor of the Lolitrem Family of Tremorgenic Mycotoxins. *J. Agric. Food Chem.* **1997**, *45*, 199–204. [CrossRef]

16. Gallagher, R.T.; Finer, J.; Clardy, J.; Leutwiler, A.; Weibel, F.; Acklin, W.; Arigoni, D. Paspalinine, a Tremorgenic Metabolite from *Claviceps paspali* Stevens Et Hall. *Tetrahedron Lett.* **1980**, *21*, 235–238. [CrossRef]

17. Sun, K.; Li, Y.; Guo, L.; Wang, Y.; Liu, P.; Zhu, W. Indole diterpenoids and isocoumarin from the fungus, *Aspergillus flavus*, isolated from the prawn, *Penaeus vannamei*. *Mar. Drugs* **2014**, *12*, 3970–3981. [CrossRef] [PubMed]

18. Fan, Y.; Wang, Y.; Liu, P.; Fu, P.; Zhu, T.; Wang, W.; Zhu, W. Indole-diterpenoids with anti-H1N1 activity from the aciduric fungus *Penicillium camemberti* OUCMDZ-1492. *J. Nat. Prod.* **2013**, *76*, 1328–1336. [CrossRef] [PubMed]

19. Belofsky, G.N.; Gloer, J.B.; Wicklow, D.T.; Dowd, P.F. Antiinsectan alkaloids: Shearinines A-C and a new paxilline derivative from the ascostromata of *Eupenicillium shearii*. *Tetrahedron* **1995**, *51*, 3959–3968. [CrossRef]

20. Harms, H.; Rempel, V.; Kehraus, S.; Kaiser, M.; Hufendiek, P.; Müller, C.E.; König, G.M. Indoloditerpenes from a marine-derived fungal strain of *Dichotomomyces cejpii* with antagonistic activity at GPR18 and cannabinoid receptors. *J. Nat. Prod.* **2014**, *77*, 673–677. [CrossRef] [PubMed]

21. Yurchenko, A.N.; Ivanets, E.V.; Smetanina, O.F.; Pivkin, M.V.; Dyshlovoi, S.A.; von Amsberg, G.; Afiyatullov, S.S. Metabolites of the Marine Fungus *Aspergillus candidus* KMM 4676 Associated with a Kuril Colonial Ascidian. *Chem. Nat. Compd.* **2017**, *53*, 747–749. [CrossRef]

22. Sallam, A.A.; Houssen, W.E.; Gissendanner, C.R.; Orabi, K.Y.; Foudah, A.I.; El Sayed, K.A. Bioguided discovery and pharmacophore modeling of the mycotoxic indole diterpene alkaloids penitrems as breast cancer proliferation, migration, and invasion inhibitors. *MedChemComm* **2013**, *4*. [CrossRef] [PubMed]

23. De Jesus, A.E.; Steyn, P.S.; van Heerden, F.R.; Vleggaar, R.; Wessels, P.L.; Hull, W.E. Tremorgenic mycotoxins from *Penicillium crustosum*. Structure elucidation and absolute configuration of penitrems B–F. *J. Chem. Soc. Perkin Trans. 1* **1983**, *41*, 1857–1861. [CrossRef]

24. De Jesus, A.E.; Steyn, P.S.; Van Heerden, F.R.; Vleggaar, R.; Wessels, P.L.; Hull, W.E. Tremorgenic mycotoxins from *Penicillium crustosum*: Isolation of penitrems A–F and the structure elucidation and absolute configuration of penitrem A. *J. Chem. Soc. Perkin Trans. 1* **1983**, *14*, 1847–1856. [CrossRef]

25. Penn, J.; Biddle, J.R.; Mantle, P.G.; Bilton, J.N.; Sheppard, R.N. Pennigritrem, a naturally-occurring penitrem A analogue with novel cyclisation in the diterpenoid moiety. *J. Chem. Soc. Perkin Trans. 1* **1992**, *23*, 23–26. [CrossRef]

26. Cutler, H.G.; Cole, R.J.; Cox, R.H.; Wells, J.M. Fungal metabolites: Interesting new plant growth inhibitors. *Proc. Plant Growth Regul. Work. Group* **1979**, *6*, 87–91.

27. Cutler, H.G.; LeFiles, J.H.; Crumley, F.G.; Cox, R.H. Hydroxyterphenyllin: A novel fungal metabolite with plant growth inhibiting properties. *J. Agric. Food Chem.* **1978**, *26*, 632–635. [CrossRef]

28. Guo, Z.K.; Yan, T.; Guo, Y.; Song, Y.C.; Jiao, R.H.; Tan, R.X.; Ge, H.M. P-terphenyl and diterpenoid metabolites from endophytic *Aspergillus* sp. YXf3. *J. Nat. Prod.* **2012**, *75*, 15–21. [CrossRef] [PubMed]

29. Mantle, P.G.; Weedon, C.M. Biosynthesis and transformation of tremorgenic indole-diterpenoids by *Penicillium paxilli* and *Acremonium lolii*. *Phytochemistry* **1994**, *36*, 1209–1217. [CrossRef]

30. Dyshlovoy, S.A.; Menchinskaya, E.S.; Venz, S.; Rast, S.; Amann, K.; Hauschild, J.; Otte, K.; Kalinin, V.I.; Silchenko, A.S.; Avilov, S.A.; et al. The marine triterpene glycoside frondoside A exhibits activity in vitro and in vivo in prostate cancer. *Int. J. Cancer* **2016**, *138*, 2450–2465. [CrossRef] [PubMed]

31. Dyshlovoy, S.A.; Venz, S.; Shubina, L.K.; Fedorov, S.N.; Walther, R.; Jacobsen, C.; Stonik, V.A.; Bokemeyer, C.; Balabanov, S.; Honecker, F. Activity of aaptamine and two derivatives, demethyloxyaaptamine and isoaaptamine, in cisplatin-resistant germ cell cancer. *J. Proteom.* **2014**, *96*, 223–239. [CrossRef] [PubMed]

32. Dyshlovoy, S.A.; Hauschild, J.; Amann, K.; Tabakmakher, K.M.; Venz, S.; Walther, R.; Guzii, A.G.; Makarieva, T.N.; Shubina, L.K.; Fedorov, S.N.; et al. Marine alkaloid monanchocidin a overcomes drug resistance by induction of autophagy and lysosomal membrane permeabilization. *Oncotarget* **2015**, *6*, 17328–17341. [CrossRef] [PubMed]